Energy Distribution of Projectile Fragment Particles in heavy Ion Therapeutic Beam

Naruhiro MATSUFUJI, Hiromi TOMURA, Yasuyuki FUTAMI, Haruo YAMASHITA,
Akifumi FUKUMURA, Tatsuaki KANAI
National Institute of Radiological Sciences (NIRS)
9-1, Anagawa-4, Inage-ku, Chiba-shi, Chiba 263-8555 JAPAN
e-mail : matufuji@nirs.go.jp

Akio HIGASHI, Takashi AKAGI
Hyogo Prefectural Government
5-10-1, Shimoyamatedori, Chuo-ku, Kobe-shi, Hyogo 650-0011 JAPAN

Hideaki KOMAMI, Toshiyuki KOHNO
Tokyo Institute of Technology
4259 Nagatsuda-cho, Midori-ku, Yokohama-shi, Kanagawa 226-0026 JAPAN

Production of fragment particles in a patient's body is one of important problems for heavy charged particle therapy. It is required to know the yield and the energy spectrum for each fragment element - so called 'beam quality' to understand the effect of therapeutic beam precisely. In this study, fragment particles produced by practical therapeutic beam of HIMAC were investigated with using tissue-equivalent material and a detector complex. From the results, fragment particles were well identified by difference of their atomic numbers and the beam quality was derived. Responses of the detectors in this energy region were also researched.

1. Introduction

High energetic heavy charged particles have many desirable characteristics for radiotherapy. What is particularly important in physical point of view is its unique depth-dose distribution known as 'Bragg curve' and less scattering in a matter. These features enable us to localize irradiation dose to tumor in deep body much better than using conventional beams as photon, neutron or even proton. The advantage is highly regarded as important especially when treating tumor grown close to critical normal tissue.

However, the heavy charged particle beam brings its specific physical problem that should be taken into consideration, *i.e.*, production of fragment particles. High energetic heavy charged particle is broken into some fragment particles in a patient's body by spallation reaction. Fig.1 shows the model of fragment reaction. The velocity of projectile fragments is nearly equal to the velocity of primary particle at the reaction point. Therefore, the projectile fragments lighter than primary particles are transported to region deeper than the range of primary particles and cause unwanted exposure to normal tissues there.

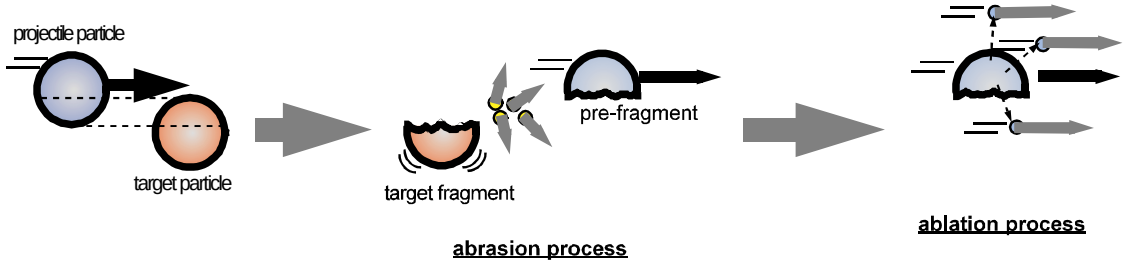

Fig.1 Spallation reaction in abrasion-ablation model [1].

The production of fragment particles also complicates biological effectiveness of the therapeutic beam because relative biological effectiveness (RBE) of radiation is a function of the beam quality: namely the kind of particle and its linear energy transfer (LET) [2]. In our treatment planning, the beam quality has not been fully taken into account yet because of the lack of reliable model and data. The aim of this study is to investigate the beam quality with using experimental methods.

2. Materials and Methods

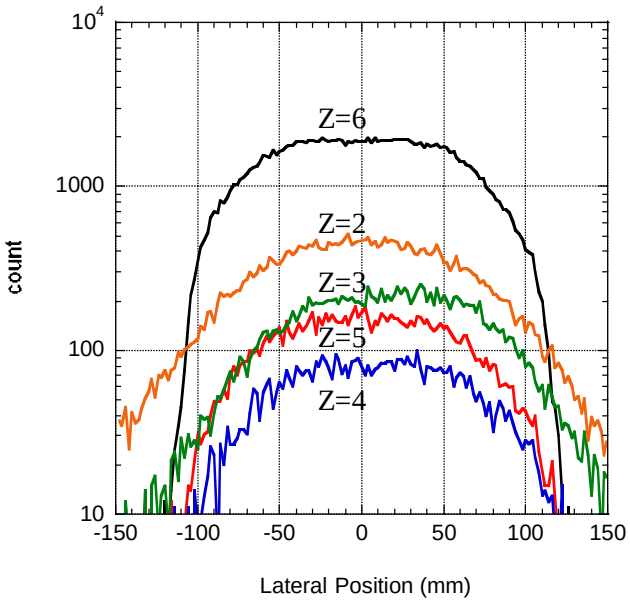

Fig.2 Lateral distribution of fragments for the incidence of 290MeV/nucleon of carbon in PMMA (90.0mm)

Experiments were carried out at biological experiment port at HIMAC (Heavy Ion Medical Accelerator in Chiba) of NIRS. Incident beam was broadened to 100 mm in diameter at iso-center with wobbler magnets and a scatterer. A stack of plates made of PMMA (polymethyl methacrylrate (Lucite), ρ=1.16g/cm^3, $(C_5H_8O_2)_n$) was used as a substitution of human body. The thickness was variously changeable in the range from 0mm to 512mm by 0.5mm step.

Lateral uniformity of the fragment element was checked by using X-ray films and a position sensitive ΔE counter. Fig.2 shows a preliminary result of fragments' lateral distribution measured by the position-sensitive counter for carbon 290 MeV/nucleon beam after passing through 90.0mm of PMMA. The result indicates sufficient uniformity at the center of the beam.

Beam quality was then investigated at the center position for 290 MeV/nucleon of carbon beam that has been used for our clinical trial. Beams of 400 MeV/nucleon of neon, 150 MeV/nucleon of helium and 490 MeV/nucleon of silicon were also used to research the responses of measurement system. These beams have the range of about 150mm in water. Intensity of the beam was drastically reduced than the intensity for therapy: in the level of 10^4 particles/3.3s at the biological port that enables us to count particles one by one.

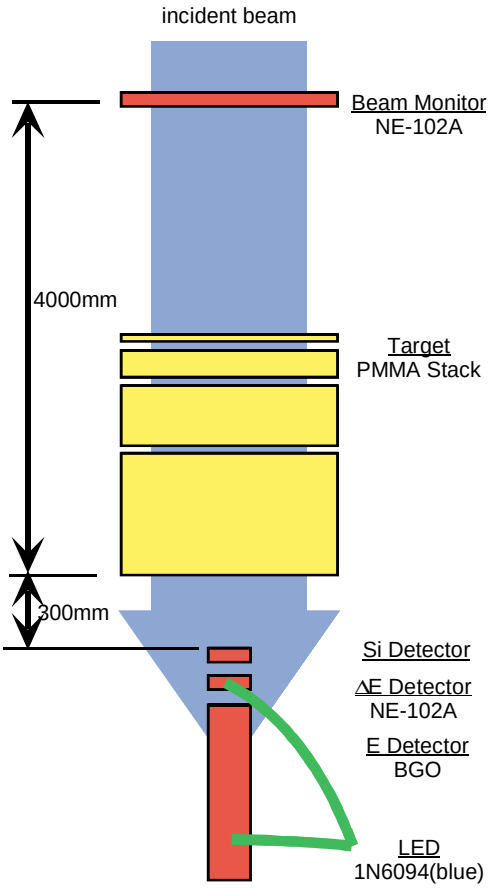

Fig.3 Configulation of beam quality measurement system.

We configured the measurement system of the beam quality based on counter telescope method. The experimental arrangement is illustrated in Fig.3. A NE102A plastic scintillator of 2.0 mm in thickness was served for counting primary particles and located at the upstream position in the experiment room. Another NE102A of 5.0 mm in thickness and 300.0 mm thickness of BGO scintillator were placed at the isocenter, 300mm downstream from PMMA target, and used as ΔE and E detector, respectively. The plastic scintillators were connected with HAMAMATSU photomultipliers while BGO scintillator was connected with HAMAMATSU photo-diode to gain wider dynamic range. A silicon detector of 1.5 mm in thickness was placed in front of ΔE detector to measure energy loss spectra. Stabilized blue light emitted by an LED was guided to the scintillators via optical cables to monitor drift of the gain. Measurements were carried out by changing the thickness of PMMA variously. Outputs from the detectors were processed with NIM modules and stored in a UNIX computer in list mode via Ethernet.

3. Results and Discussion

3-1 Particle Distribution

Fragment particle was well identified down to hydrogen by ΔE-E scatter plot of the NE102A and the BGO scintillator. Fig.4 shows an example of the scatter plot for 400 MeV/nucleon of neon beam after passing through 135.0 mm of PMMA target. The number of particles included in each band were counted and normalized by total number of incident primary particles. Fig.5 and 6 shows the number of primary carbon and fragment particles for each element as a function of PMMA thickness. Lines in the figure represent calculational results of 'hibrac' [3]. They shows good agreement on primary carbon particles, however, discrepancy is also shown on the number of hydrogen or beryllium particles. The reason is considered as an incompleteness of cross section model in the code.

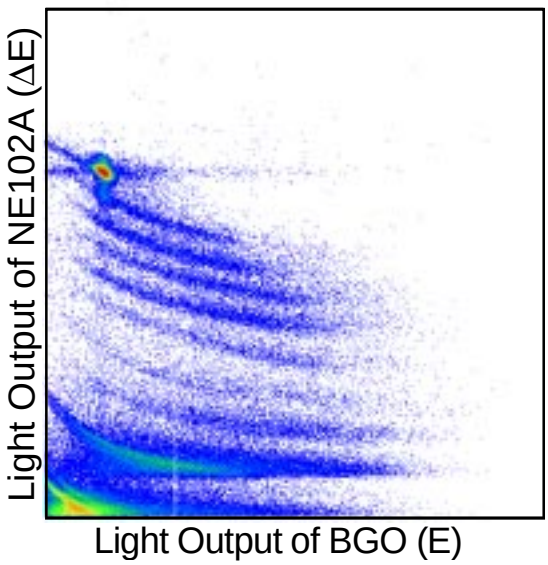

Fig.4 DE-E scatter plot for the incidence of 400MeV/nucleon of neon in PMMA (135.0mm).

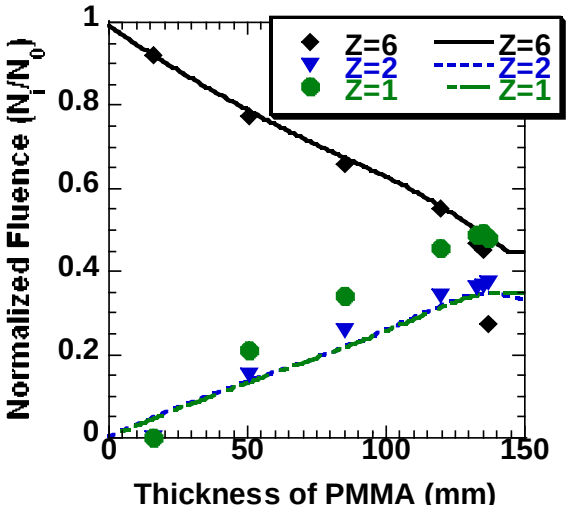

Fig.5 Fluence of primary and fragments (Z=1, 2) as a function of PMMA thickness for the incidence of 290 MeV/nucleon of carbon.

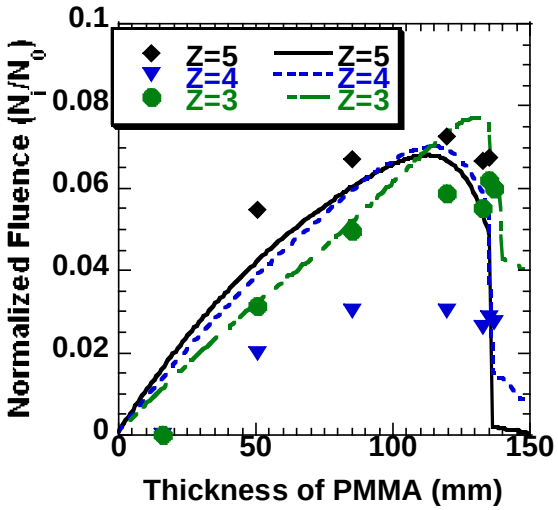

Fig.6 Fluence of fragments (Z=3–5) as a function of PMMA thickness for the incidence of 290 MeV/nucleon of carbon.

3-2 Response Function and Energy Spectra

The responses of silicon detector, NE102A scintillator and BGO scintillator in this energy region were determined as shown in figs. 7-9, respectively. The response of the silicon detector can be regarded as independent of the kind of elements. The characteristic enables us to obtain energy loss in silicon detector in good precision. However, the atomic number of silicon is larger than water that accupies the main component of

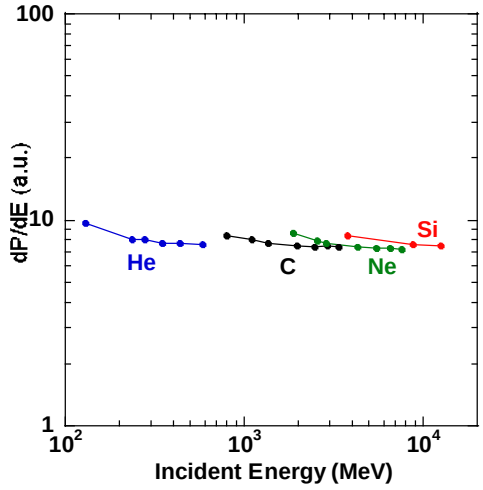

Fig.7 Response function of silicon detector.

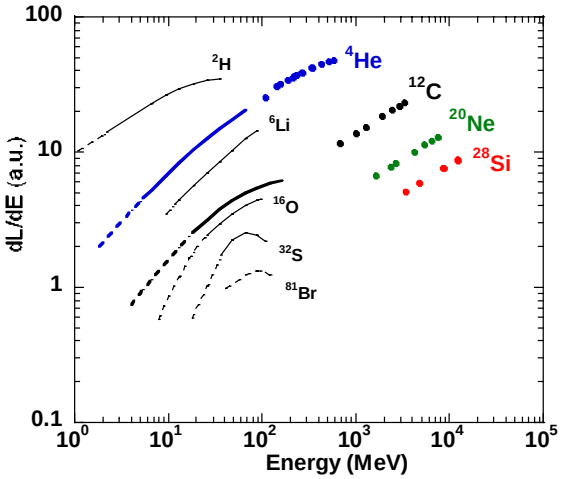

Fig.8 Response function of NE102A detector.
lines : Becchetti *et al*[4], dots : this work

human tissue. The large difference of atomic number makes it difficult to deduce energy loss in tissue because the stopping power drastically changes by the difference of atomic number.

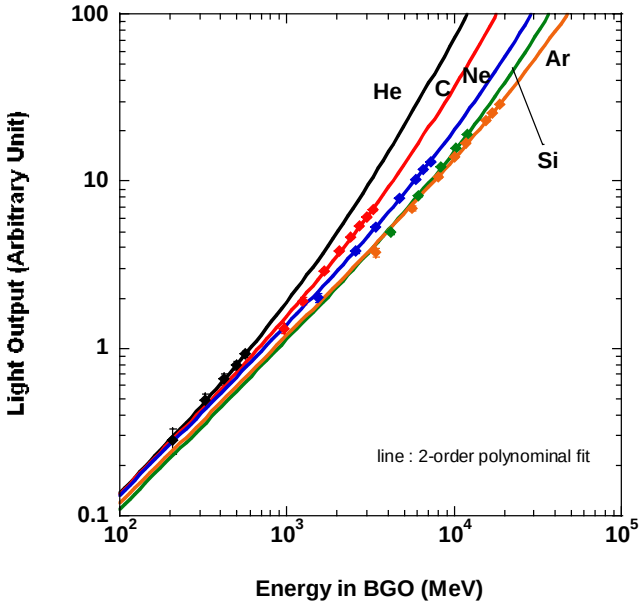

Fig.9 Response function of BGO scintillator.

The responses of NE102A plastic scintillators show obvious element dependency in this energy region. As shown in fig.5, the yields of lighter elements such as hydrogen or proton in patient's body are very large in comparison with other elements. The response means an advantage to identify these lighter elements by using NE102A scintillator as ΔE detector because the element dependency tends to enlarge the difference of DE/dx of lighter elements.

The response of BGO scintillator also shows element dependency. Here, unlike energy loss spectra in silicon, the residual energy spectra in BGO are independent of the kind of medium. Therefore, the information is directly applicable as basic data to the estimation of biological effect of

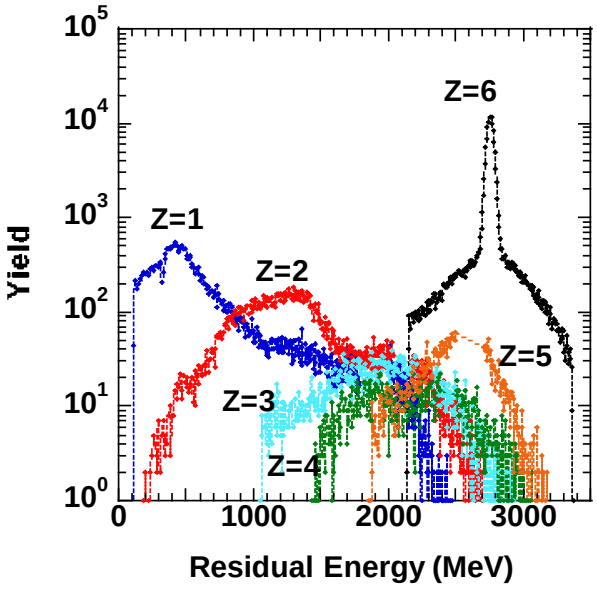

Fig.10 Energy spectra of fragments for the incidence of 290 MeV/nucleon of carboon in PMMA (40.0mm) .

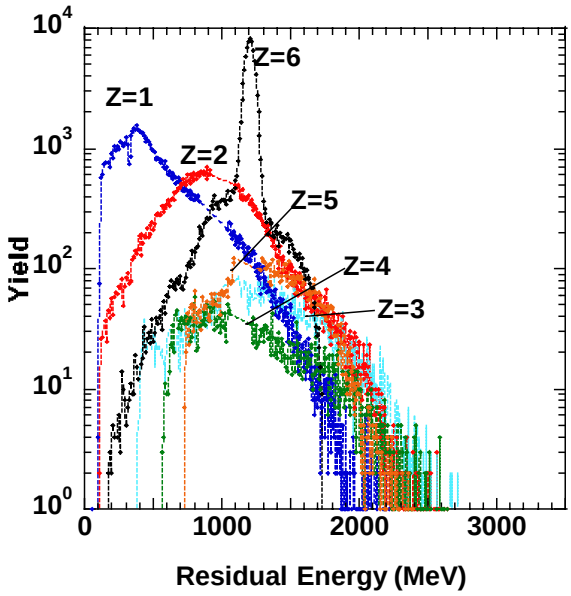

Fig.11 Energy spectra of fragments for the incidence of 290 MeV/nucleon of carboon in PMMA (120.0mm) .

therapeutic beam. Fig.10 and 11 shows preliminary spectra of residual energy of carbon beam deduced from BGO's energy response function.

4. Conclusion

Beam quality measurement system was developed. Through the measurements, fragment particles were well identified by difference of their atomic numbers. The comparison of the yield of fragments with calculational result showed differences on hydrogen and beryllium. It is strongly required to establish reliable simulation code together with experimental data from now on.

Responses of the detectors in this energy region were determined. The results extended existing measured responses. Appropriate usage of each detector for the beam quality measurement was derived based on the each detector's response function.

Acknowledgements

Authors wish to thank to the members of division of accelerator physics and engineering and all the staffs who take part in HIMAC project for their kind supports.

References

[1] Wilson J.W., Townsend L.W. and Badavi F.F., Nucl. Instr. and Meth. Phys. Res. Sect. B, B18, 225(1987)

[2] Kiefer J.: Int'l. J. of Radiat. Biol., 48, 873 (1986)

[3] Sihver L., Tsao C.H., Silberberg R., Barghouty A.F. and Kanai T.: Adv. Space Res., 17, 105 (1995)

[4] Becchetti F.D., Thorn C.E. and Levine M.J.: Nucl. Instr. and Meth., 138, 93 (1976)

【和文】

治療領域の重粒子線から生じる入射核フラグメントのエネルギー分布

松藤成弘、外村浩美、二見康之、山下晴男、福村明史、金井達明
放射線医学総合研究所
〒263-8555 千葉市稲毛区穴川４－９－１
電子メール matufuji@nirs.go.jp

東明男、赤城卓
兵庫県庁
〒650-0011 神戸市中央区下山手通 5-10-1

駒見英明、河野俊之
東京工業大学
〒226-0026 横浜市緑区長津田町 4259